Journal of Computers Vol. 29 No. 4, 2018, pp. 12-30
doi:10.3966/199115992018082904002

Intensity-based Co-occurrence Local Ternary Patterns for Image Retrieval

Li Li[1,2], Lin Feng[1,3*], Sheng-Lan Liu[4], Mu-Xin Sun[3], Jun Wu[3], Hui-Bing Wang[1]

[1] School of Computer Science and Technology, Faculty of Electronic Information and Electrical Engineering, Dalian University of Technology, Dalian 116024, China
hdlili@126.com, fenglin@dlut.edu.cn, whb08421005@mail.dlut.edu.cn

[2] School of Information and Electrical Engineering, Hebei University of Engineering, Handan 056038, China

[3] School of Innovation and Entrepreneurship, Dalian University of Technology, Dalian 116024, China
{111111, shuxuewujun}@mail.dlut.edu.cn

[4] School of Control Science and Engineering, Faculty of Electronic Information and Electrical Engineering, Dalian University of Technology, Dalian 116024, China
liusl@mail.dlut.edu.cn

Received 15 November 2016; Revised 7 March 2017; Accepted 30 March 2017

Abstract. Feature descriptors based on local pattern have been applied successfully in image retrieval due to their simplicities. However, most of the local pattern methods only consider the relationships between the center pixel and its boundary pixels. And these methods disregard the co-occurrences between patterns in images. In this paper, we propose a novel feature extraction algorithm called intensity-based co-occurrence local ternary patterns (CLTP) using HSV color space. The brightness level at a center pixel is highly dependent on the brightness levels of its neighbors. The neighbors intensity (NI) for a given center pixel are considered in CLTP and an operator, namely NI-CLTP, is proposed. HSV color space is used in this algorithm to extract color information. NI-CLTP encodes the intensity co-occurrence of similar ternary edges among the surrounding neighbors for a given center pixel in an image and it is different from the existing local pattern methods. Furthermore, NI-CLTP is combined with Gabor transform to extract effective texture feature. Extensive experiments on diverse databases verify the effectiveness of our proposed method.

Keywords: co-occurrence local ternary patterns, Gabor transform, image retrieval, local binary pattern, local ternary pattern

1 Introduction

In recent years, with the growth of network technology and multimedia technology, the size of image databases is increasing rapidly. It is an extremely difficult task to search and retrieve images from a huge database. Therefore, image retrieval has become an important topic in pattern recognition and image processing. At present, most of web search engines (such as Google and Baidu) can retrieve images using keywords. However, text based retrieval methods have two drawbacks. Firstly, images are annotated by human labor and it is time-consuming for a large volume of image database. Secondly, the retrieval results are inaccurate, because different annotators tend to use different ways to handle the same image. To overcome these problems, the content-based image retrieval (CBIR) is proposed. CBIR [1-4] first extracts the visual low-level features (such as color, texture, shape, etc.) which can represent an image, and then computes the similarities between the query image and images in the database. Finally, the top-N images will be displayed by distance measure. Feature extraction is a critical step for retrieving the

* Corresponding Author

images from a huge database and the performance of low-level features directly impacts the results of image retrieval.

Color and texture are two important visual features in CBIR. Diverse methods have been proposed to extract the color and texture features for image retrieval. Color presents the intensity distribution in different color channels. The important color descriptors are color histogram, color moments, color correlograms and color coherence vector. Color histogram is invariant to scale and orientation and it is widely applied for image retrieval [5]. However, color histogram lacks spatial information. Therefore, color moments [6], color correlograms [7] and color coherence vector [8] have been proposed to exploit the spatial information. Sticker et al. proposed color moments which considered the spatial position information. However, color moments consume a lot of computation space. Color correlograms were proposed that characterize the spatial correlation between pair of colors. Color coherence vector was introduced for image retrieval which incorporated spatial information of images. Texture describes the information of the coarseness and repetitive patterns of objects. Many texture descriptors have been proposed to describe image features. Gabor wavelet transformation has been widely applied in computer vision [9-10]. The scale-invariant and rotation-invariant Gabor transform features were extracted for image retrieval by Han et al. [11]. Gray level co-occurrence matrix (GLCM) was introduced to describe texture feature using the co-occurrence relationship of pixels in images [12-16]. Siqueira et al. [17] extended the GLCM to multi-scale descriptors for texture description.

Many local patterns have been proposed for image retrieval, texture classification, face recognition, etc. Viola et al. [18] introduced Haar features for real-time face detection. Ojala et al. [19] presented local binary patterns (LBP) for image texture classification. Subsequently many variants related to LBP have been presented for texture analysis, face recognition, face recognition [20], palmprint recognition, etc. Heikkilä et al. [21] proposed center symmetric local binary pattern (CS-LBP) which compared center-symmetric pairs of pixels. Tan et al. [22] presented local ternary patterns (LTP) for face recognition which extends LBP to 3-valued codes. Local configuration pattern (LCP) has been combined with LBP for texture classification [23]. Guo et al. [24] proposed completed local binary pattern (CLBP), which integrated CLBP_Center (CLBP_C), CLBP_Sign (CLBP_S) and CLBP_Magnitude (CLBP_M) into joint histogram for texture classification. Local mesh patterns (LMP) [25] encoded the relationship among the surrounding neighbors for a given center pixel in an image for biomedical image indexing and retrieval.

Most of the techniques in CBIR have used a single feature during the last decade. However, a single feature usually has some limitations. It is difficult to use single property to represent various image contents. There are some methods that fuse color and texture features. Shen et al. [26] combined color, texture and spatial structure for image representation. Images were segmented into small regular regions and then extracted local color, texture and census transform histogram (CENTRIST) respectively. Liu et al. [27] proposed multi-texton histogram (MTH) that integrates the advantages of co-occurrence matrix and histogram to characterize color and texture features. ElAlami [28] exploited Gabor filter and 3D color histogram for image retrieval.

Many local patterns have been proposed and these methods are used in image retrieval. However, most of the local patterns only consider the relationships between a given center pixel and its neighbors in the alone pattern, and these methods lose local textural information regarding the co-occurrence of patterns in an image.

In this paper, we address the co-occurrence of similar local patterns. The main contributions of our method are summarized as follows:

(1) We propose a novel neighbors intensity co-occurrence local ternary patterns (NI-CLTP) feature descriptor. NI-CLTP codes the co-occurrence between adjacent local patterns, while traditional local patterns lose the co-occurrence of patterns.

(2) We further extend NI-CLTP to neighbors intensity Gabor co-occurrence local ternary patterns (NI-GCLTP) by Gabor filters, in which extracts different scales and orientations texture information.

(3) For a given pixel, NI-CLTP is calculated by the threshold of neighbors with the average gray level of surrounding neighbors. This selection of threshold is more robust than the center pixel of LBP.

(4) We extract color and texture feature to represent images, while traditional local patterns methods disregard the description of color information.

(5) We evaluate the proposed method on Corel-1000, Corel-5000 and Corel-10000 databases, and experimental results demonstrate the effectiveness of the proposed method in CBIR.

The remainder of this paper is organized as follows. In Section 2, color space, LBP and LTP are

introduced. Section 3 presents co-occurrence local ternary patterns (CLTP) scheme. The proposed system framework is illustrated in Section 4. Experimental results and discussions are illustrated in Section 5. Finally, Section 6 concludes the paper.

2 Color and Texture Descriptors

Before discussing the proposed method in detail, this section gives brief reviews of color quantization in HSV color space, the local binary pattern (LBP) and local ternary pattern (LTP).

2.1 Color Quantization in HSV Color Space

There are already many excellent color space models [29], such as RGB, Lab, YIQ, HSV, etc. It has been suggested that color space plays an important role on the performance of image representations. The HSV color space [30] is very close to the human visual perception system and it is widely applied for color feature extraction. H, S and V components represent hue, saturation and value information in HSV color space respectively, $H \in [0,360], S \in [0,1], V \in [0,1]$. H component is measured by an angle value from 0° to 360° and different angles present different colors. S component is numbered from 0 to 1, as saturation varies from low to high, the color saturation increases. V component also varies from 0 to 1. To extract discriminative information, HSV color space is adopted for image representation in this work. To reduce the computational complexity, it is necessary to make appropriate color space quantization. In our paper, H and S components are quantized into 72 and 20 bins.

2.2 Local Binary Pattern (LBP)

The local binary pattern is encoded by comparing a given center pixel with its neighbors. LBP takes P points around the center pixel as neighbors, the gray values of its neighbors are $g_0, g_1, \cdots, g_{P-1}$. The spatial structure in the neighborhood is interpreted as a P-bit binary number by comparing the center pixel with its neighbors, which can be defined as follows:

$$LBP_{P,R} = \sum_{m=0}^{P-1} s(g_m - g_c)2^m \tag{1}$$

$$s(x) = \begin{cases} 1, & if\ x \geq 0 \\ 0, & else \end{cases} \tag{2}$$

where P denotes the number of neighbors, and R is the radius of the circle defining the neighborhood. g_c denotes the gray-value of the center pixel.

2.3 Local Ternary Pattern (LTP)

Based on the basic idea in LBP, LTP [22] was designed to adopted 3-valued codes to describe the neighboring relationship among pixels, in which gray-levels in the zone of width $\pm t$ around g_c are quantized to 0, those above ($g_c + t$) are quantized to $+1$, those below ($g_c - t$) are quantized to -1. The LBP code is replaced by a ternary LTP code and the LTP is defined as follows:

$$s'(x, g_c, t) = \begin{cases} 1, & x \geq g_c + t \\ 0, & |x - g_c| < t \\ -1, & x \leq g_c - t \end{cases} \tag{3}$$

where t is a user-specified threshold.

To facilitate the following discussion, we set the number of neighbors as 8 and the radius of the circle defining the neighborhood as 1.

The above methods of the local patterns only consider the relationships between a given center pixel and its neighbors in the alone pattern, and the correlation between adjacent patterns in images is

overlooked. The co-occurrence between patterns can extract more discriminative information than alone pattern without spatial correlation. Therefore, we consider the co-occurrence of similar adjacent patterns in this paper to get a discriminative texture feature.

3 Co-occurrence Local Ternary Patterns (CLTP)

3.1 NI-CLTP Descriptor

In an image, the brightness level at a point is highly dependent on the brightness levels of its neighbors unless the image is simply random noise [31]. Inspired by this idea, Liu et al. [32] proposed the intensity-based features which considered the intensities of neighbors (NI-LBP). However, NI-LBP does not reveal any information regarding the co-occurrence of patterns in the image.

The idea of LBP, LTP and the co-occurrence matrix features have motivated us to propose the co-occurrence local ternary patterns (CLTP) for image retrieval. In CLTP, we consider neighbors intensity (NI) for a given center pixel. So the novel descriptor is named as NI-CLTP. Co-occurrence matrix features have motivated us to consider the co-occurrence information between patterns. There are three pixel pairs $(x,y)=(1,1)$, $(x,y)=(0,0)$ and $(x,y)=(0,1)$ or $(x,y)=(1,0)$ between adjacent local binary patterns in a local image patch. The co-occurrence of three pixel pairs can just use the ternary coding by the idea of LTP. Therefore, we code co-occurrence pixel pairs by using 3-valued (1,2,0) and the ternary coding scheme is similar to the coding scheme of LTP.

NI-CLTP is calculated based on the co-occurrence of similar ternary edges among the surrounding neighbors for a given center pixel in eight directions as shown in Fig. 1. The co-occurrence among the surrounding neighbors are calculated based on the relationships between neighbors with the average gray value of neighbors (we use the average gray value of neighbors which can be found in Ref. [32]). To facilitate discussion, we set used parameters as: $P=8$, $R=1$ in the NI-CLTP.

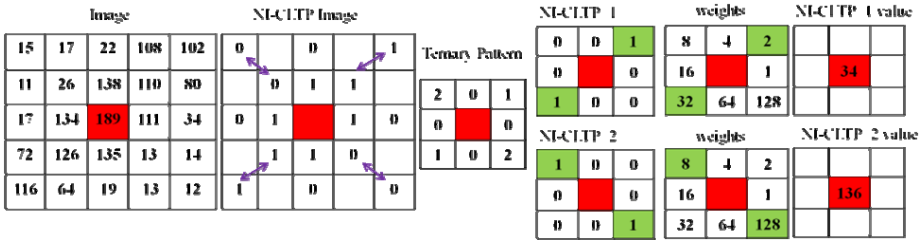

Fig. 1. Example for NI-CLTP calculation (two average gray values of neighbors in R and $R+1$ along eight directions are 99.13 and 42.13)

NI-CLTP for a given center pixel is calculated by using intensity distributions of its neighbors as follows:

$$T_{P,R}(g_m)=I_{P,R}(g_m)-t;\ \ m=1,2,\cdots,P \tag{4}$$

where $P=8$ is the number of neighbors, $R=1$ is the radius of the neighborhood, the gray values of the surrounding neighbors are $I_{P,R}(g_m)$, and $t=\frac{1}{8}\sum_{m=1}^{P} I_{P,R}(g_m)$.

$$T_{P,R+1}(g_m)=I_{P,R+1}(g_m)-\tilde{t};\ \ m=1,2,\cdots,P \tag{5}$$

where the gray values of the surrounding neighbors are $I_{P,R+1}(g_m)$, and $\tilde{t}=\frac{1}{8}\sum_{m=1}^{P} I_{P,R+1}(g_m)$.

After calculating the intensity distributions of the surrounding neighbors, we code them based on the indicator $s(x)$ as follows:

$$T^{1}_{P,R}(g_m)=s(T_{P,R}(g_m)) \tag{6}$$

$$T^1_{P,R+1}(g_m) = s(T_{P,R+1}(g_m)) \tag{7}$$

Then $T^1_{P,R}(g_m)$ and $T^1_{P,R+1}(g_m)$ are coded as ternary values. NI-CLTP is calculated based on the co-occurrence of these ternary values as follows:

$$NI-CLTP = \begin{bmatrix} s_1(T^1_{P,R}(g_1), T^1_{P,R+1}(g_1)), \\ s_1(T^1_{P,R}(g_2), T^1_{P,R+1}(g_2)), \cdots \\ \cdots, s_1(T^1_{P,R}(g_P), T^1_{P,R+1}(g_P)) \end{bmatrix} \tag{8}$$

$$s_1(x,y) = \begin{cases} 1, & if\ x = y = 1 \\ 2, & if\ x = y = 0 \\ 0, & else \end{cases} \tag{9}$$

NI-CLTP is a 3-valued codes (1,2,0) which is converted into two binary patterns.

Using this method, 2×2^P distinct values can be obtained for the NI-CLTP code. In order to reduce the computational cost, we use the uniform patterns [33] in this work. The uniform pattern is the number of bitwise transitions from 1 to 0 or vice versa and its uniformity measure is at most 2, other patterns are non-uniform. For instance, the patterns 00000000 and 11001111 are uniform, while 00100100 and 01010010 are non-uniform patterns. The uniform patterns produce 59 output labels for neighbors of 8 sampling points. Thus, the feature vector length of NI-CLTP is $2 \times 59 = 118$.

3.2 Analysis

For a given center pixel, NI-CLTP code is computed by comparing its neighbors with the average gray level of its neighbors. Then NI-CLTP encodes the co-occurrence of 3-valued edges in eight directions. Finally, a 3-valued codes is converted into two binary patterns ($NI-CLTP\_1$ and $NI-CLTP\_2$). Fig. 2 takes a image from Corel-10000 database as an example to show the feature extraction process of NI-CLTP.

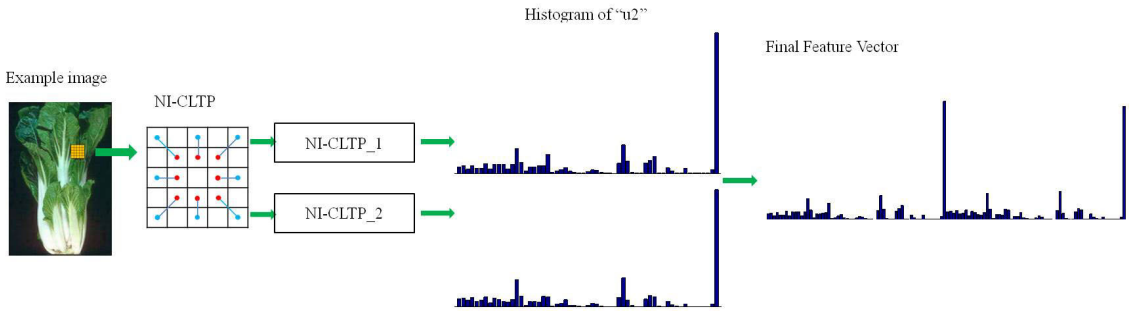

Fig. 2. Feature vector generation for a given sample image based on NI-CLTP

Fig. 3 shows the comparison between LBP and NI-CLTP on a 5×5 sample image patch. Two average gray values of local neighbors in $R = 1$ and $R + 1 = 2$ along eight directions are 99.13 and 42.13. From Fig. 3, we can see that LBP does not match the visual patterns. In contrast, NI-CLTP outputs co-occurrence visual patterns. Therefore, NI-CLTP preserves more weak edge information than LBP.

3.3 Multi-scale Feature Extraction

Gabor transform (GT) has been widely used in texture analysis. Joint LBP and GT have been proven to be an effective method for face recognition [34]. The idea of GT has motivated us to propose Gabor co-occurrence local ternary patterns (GCLTP) for image retrieval. In GCLTP, we also consider neighbors intensity (NI) for a given center pixel. So the novel descriptor is named as NI-GCLTP. We choose Gabor filters in different scales and orientations to process images.

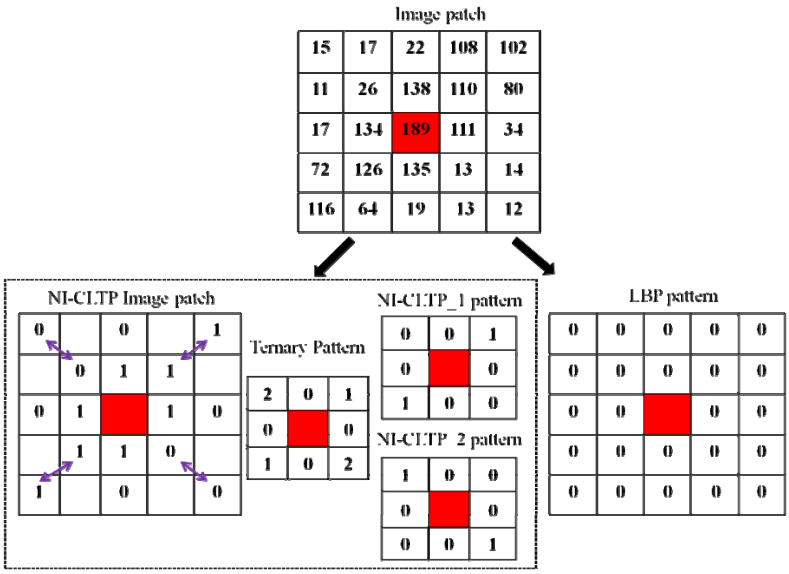

Fig. 3. Comparison of LBP and NI-CLTP on a sample image patch

In this work, all filter parameters are set as the spatial implementation of Gabor transform [35]. A 2-D Gabor function can be defined as follows:

$$f(x,y)=\frac{1}{2\pi\sigma_x\sigma_y}e^{\left[-(1/2)\left(x^2/\sigma_x^2+y^2/\sigma_y^2\right)+2\pi j\omega x\right]} \tag{10}$$

where σ_x and σ_y represent the standard deviations of the Gaussian envelope, ω represents the frequency of sinusoid.

The Gabor filters can be expressed in multiple orientations and scales as follows:

$$f_{s,d}(x,y)=t^{-s}f(\tilde{x},\tilde{y}) \tag{11}$$

Where $\tilde{x}=t^{-s}(x\cos\theta+y\sin\theta)$, $\tilde{y}=t^{-s}(-x\sin\theta+y\cos\theta)$, $s\in\{0,1,\cdots,S-1\}$ and $d\in\{0,\cdots,D-1\}$ represent the scale and orientation. S and D are the number of scales and orientations, respectively. $\theta=d\pi/D$, $t=(H/L)^{-1/S-1}$, H and L are the upper and lower bound of the frequency band, $H=0.49$, $L=0.05$. The variables in Eq. (10) and Eq. (11) are defined as follows:

$$\omega_{s,d}=H,\ \sigma_{x,s,d}=\frac{(t+1)\sqrt{2\ln 2}}{2\pi t^s(t-1)L},\ \sigma_{y,s,d}=\frac{1}{2\pi\tan(\frac{\pi}{2D})\sqrt{\frac{H^2}{2\ln 2}-(\frac{1}{2\pi\sigma_{x,s,d}})^2}}$$

The response of the Gabor filter is given by the convolution of the Gabor window with a given image I as follows:

$$F_{s,d}(x,y)=\sum_u\sum_v I(x-u,y-v)f_{s,d}(u,v) \tag{12}$$

In this work, we choose Gabor filters in three scales and four directions $(0^\circ,45^\circ,90^\circ,135^\circ)$ to process a given image. Fig. 4 shows the feature extraction process of NI-GCLTP for a filtered image.

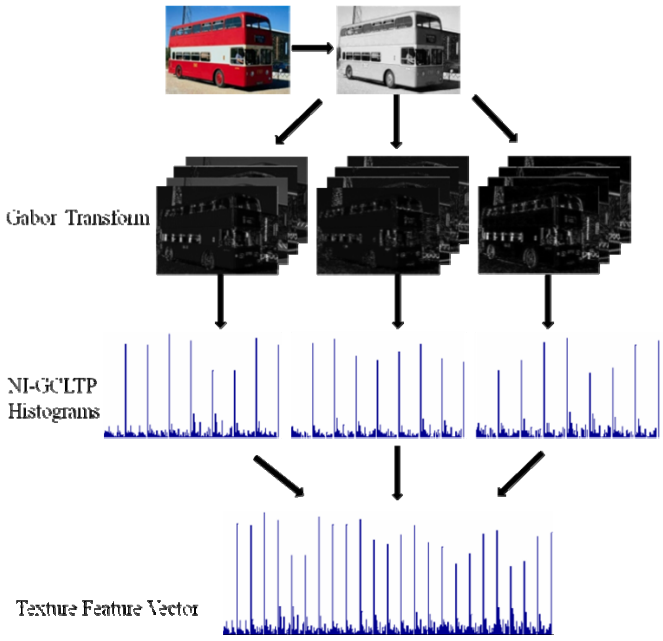

Fig. 4. The feature extraction process of NI-GCLTP for a filtered image

For a given center pixel, the NI-GCLTP is calculated by using intensity distributions of its neighbors for a filtered image as follows:

$$\tilde{F}_{P,R,s,m}(g_c)\big|_{P=8,R=1} = \begin{cases} F_{P,R,s,d}(g_m)\big|_{d=0^\circ} - t_1; & m=1 \\ F_{P,R,s,d}(g_m)\big|_{d=45^\circ} - t_1; & m=2 \\ F_{P,R,s,d}(g_m)\big|_{d=90^\circ} - t_1; & m=3 \\ F_{P,R,s,d}(g_m)\big|_{d=135^\circ} - t_1; & m=4 \\ F_{P,R,s,d}(g_m)\big|_{d=0^\circ} - t_1; & m=5 \\ F_{P,R,s,d}(g_m)\big|_{d=45^\circ} - t_1; & m=6 \\ F_{P,R,s,d}(g_m)\big|_{d=90^\circ} - t_1; & m=7 \\ F_{P,R,s,d}(g_m)\big|_{d=135^\circ} - t_1; & m=8 \end{cases} \quad \textbf{(13)}$$

where $t_1 = \frac{1}{8}\sum_{m=1}^{P} F_{P,R,s,d}(g_m)$. For a given center pixel, $F_{P,R,s,d}(g_m)$ represents the GT response at its neighbors.

$$\tilde{F}_{P,R+1,s,m'}(g_c)\big|_{P=8,R=2} = \begin{cases} F_{P,R+1,s,d}(g_{m'})\big|_{d=0^\circ} - t_2; & m'=1 \\ F_{P,R+1,s,d}(g_{m'})\big|_{d=45^\circ} - t_2; & m'=2 \\ F_{P,R+1,s,d}(g_{m'})\big|_{d=90^\circ} - t_2; & m'=3 \\ F_{P,R+1,s,d}(g_{m'})\big|_{d=135^\circ} - t_2; & m'=4 \\ F_{P,R+1,s,d}(g_{m'})\big|_{d=0^\circ} - t_2; & m'=5 \\ F_{P,R+1,s,d}(g_{m'})\big|_{d=45^\circ} - t_2; & m'=6 \\ F_{P,R+1,s,d}(g_{m'})\big|_{d=90^\circ} - t_2; & m'=7 \\ F_{P,R+1,s,d}(g_{m'})\big|_{d=135^\circ} - t_2; & m'=8 \end{cases} \quad \textbf{(14)}$$

where $t_2 = \frac{1}{8}\sum_{m'=1}^{P} F_{P,R+1,s,d}(g_{m'})$. For a given center pixel, $F_{P,R+1,s,d}(g_{m'})$ represents the GT response at its neighbors.

After calculating the intensity distributions of the surrounding neighbors, we code them based on the indicator $s(x)$ as follows:

$$f^1_{P,R,s,m}(g_m)|_{m=1,2,\cdots,8} = s(\tilde{F}_{P,R,s,m}(g_m)) \tag{15}$$

$$f^1_{P,R+1,s,m'}(g_{m'})|_{m'=1,2,\cdots,8} = s(\tilde{F}_{P,R+1,s,m'}(g_{m'})) \tag{16}$$

NI-GCLTP is defined as follows:

$$\mathrm{NI-GCLTP}_s = \begin{bmatrix} s_1(f^1_{P,R,s,1}(g_1), f^1_{P,R+1,s,1}(g_1)), \\ s_1(f^1_{P,R,s,2}(g_2), f^1_{P,R+1,s,2}(g_2)), \cdots \\ \cdots, s_1(f^1_{P,R,s,m}(g_m), f^1_{P,R+1,s,m'}(g_{m'})) \end{bmatrix} \tag{17}$$

Then NI-GCLTP is converted into two binary patterns for each scale as similar to the NI-CLTP. Finally, the histograms of NI-GCLTP are constructed for different scales (as shown in Fig. 4).

4 Proposed System Framework

In this work, we propose a novel image feature representation method, namely NI-CLTP, which represent color and texture features using the HSV color space. HSV color space is used, because it is suitable to mimic the visual system of human. In the HSV color space, H and S component histograms aim to extract global color image information. In order to extract reasonable information, we set H component as 18, 36 and 72 bins and S component as 10 and 20 bins. And V component is employed to extract texture feature because V component in HSV color space is very close to the gray level image conversion of the RGB image. NI-CLTP extracts the correlation of local neighborhood distributions for reference pixel in eight directions and preserves correlation among patterns, while conventional local patterns only extract relationships between the given center pixel and its surrounding neighbors. So NI-CLTP gets more information regarding to the correlation of pixels. Regarding the selection of the threshold, average gray values of local neighbors is more robust than gray value of the center pixel.

4.1 Proposed Image Retrieval System

In this paper, the flowchart of the proposed retrieval system framework can be seen in Fig.5 and algorithm is represented as follows.

Algorithm: *Proposed retrieval system*

Input: Query image.
Output: Retrieval results.
Step 1. Submit query image and convert color space.
Step 2. Quantize the H component and the S component and construct the histograms for color feature.
Step 3. Process images by the Gabor filter and apply NI-GCLTP on the V component.
Step 4. Construct the histogram for NI-GCLTP in three scales and four directions.
Step 5. Construct the final feature vector by concatenating the histograms of Step 2 and Step 4.
Step 6. Compare the query image with database images using similarity distance metric.
Step 7. Sort the top images and output the best matches as final results.

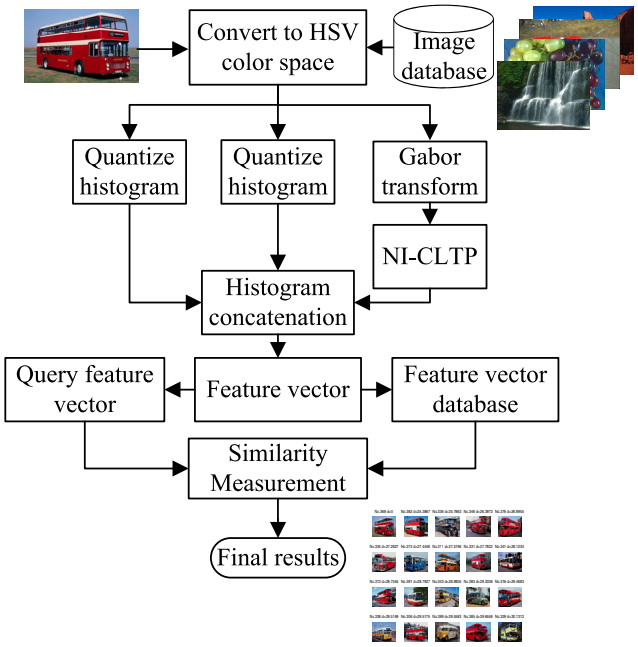

Fig. 5. Flowchart of the proposed retrieval system framework

4.2 Advantage of Proposed Scheme

(1) The proposed method considers the co-occurrence of local neighborhood distributions. However, conventional methods only simply consider the relationships between the center pixel and its neighborhoods using histogram and these methods only consider the relationship of the alone pattern. These methods do not consider any information regarding the co-occurrence of similar edges patterns in the image.

(2) As explained in Section 2.1, HSV color space is better than RGB color space and it has been proved by experiments. H and S components are used to extract global color information, and the combination of NI-CLTP and Gabor transform is applied to extract texture feature on V component.

4.3 Similarity Measure

Good feature representation and similarity measures are two crucial factors in CBIR which directly impact image retrieval precision. In this work, several common similarity measures have been used for the similarity match, including L_2 distance, L_1 distance, weighted L_1 distance and improved Canberra distance as mentioned in [36-38]. Let $Y=[y_1, y_2, \cdots, y_n]$ be the feature vector of a query image and $X=[x_1, x_2, \cdots, x_n]$ be the feature vector of each image in the database, their similarity measures can be represented as follows:

$$L_2 \text{ distance: } D(X,Y)=(\sum_{i=1}^{n}(x_i-y_i)^2)^{1/2} \tag{18}$$

$$L_1 \text{ distance: } D(X,Y)=\sum_{i=1}^{n}|x_i-y_i| \tag{19}$$

$$\text{weighted } L_1 \text{ distance: } D(X,Y)=\sum_{i=1}^{n}\frac{|x_i-y_i|}{1+x_i+y_i} \tag{20}$$

$$\text{improved Canberra distance: } D(X,Y)=\sum_{i=1}^{n}\frac{|x_i-y_i|}{|x_i+u_x|+|y_i+u_y|} \tag{21}$$

where $u_x = \sum_{i=1}^{n} \frac{x_i}{n}$, $u_y = \sum_{i=1}^{n} \frac{y_i}{n}$. n is the length of feature vector.

5 Experimental Results and Analysis

In order to analyze the performance of proposed method for image retrieval, several experiments were conducted on three databases. The same preprocessing and color quantization (72 bins for H component, 20 bins for S component and the dimension of V component is the feature vector length of GLBP, GLCP, GCSLBP, GCLBP, GLTP and GLMP) for those selected methods have been made to fairly evaluate the performance of proposed method. The abbreviations of different methods have been given in Table 1.

Table 1. Abbreviations of different methods

Abbreviations	Different methods
HSV(72-20-708)GLBP	local binary pattern with Gabor transform using HSV color space
HSV(72-20-972)GLCP	local configuration pattern with Gabor transform using HSV color space
HSV(72-20-192)GCSLBP	center symmetric LBP with Gabor transform using HSV color space
HSV(72-20-1416)GCLBP	completed LBP(CLBP_S_M) with Gabor transform using HSV color space
HSV(72-20-1416)GLTP	local ternary patterns with Gabor transform using HSV color space
HSV(72-20-2124)GLMP	local mesh patterns with Gabor transform using HSV color space

5.1 Databases

In our experiments, we apply the Corel database which is commonly used in the field of image retrieval. All images of Corel databases come from the Corel Gallery Magic 200,000 (8CDs) database which contains various contents images. Three Corel databases are used which are shown in Fig. 6. The first database is the Corel-1000 database [39] which consists 1000 images of size 256×384 or 384×256 in JPG format and is divided into 10 different categories. The second database is Corel-5000 database which contains 5000 images in 50 categories. Size of images is either 192×128 or 128×192 in JPEG format. The third database is Corel-10000 database [40] which consists 10000 images in 100 categories.

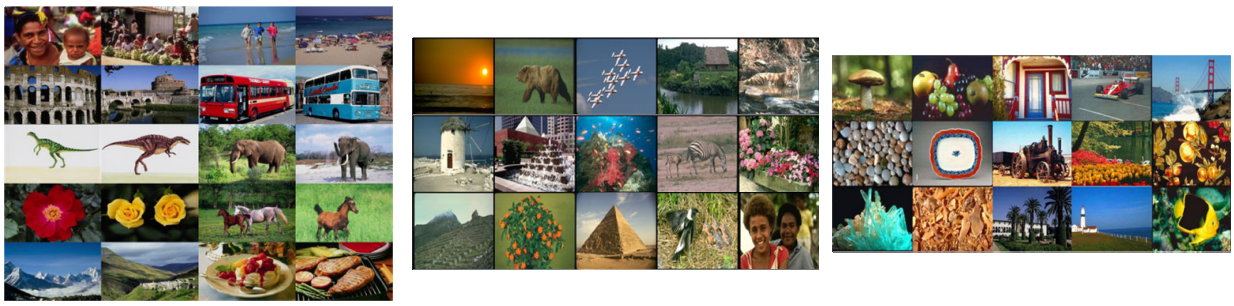

(a) Corel-1000 database (b) Corel-5000 database (c) Corel-10000 database

Fig. 6. Some sample images of three Corel databases

5.2 Performance Evaluation Metrics

The precision and recall are used to validate the performance of algorithm in image retrieval [41]. Precision is calculated as the ratio between the number of relevant images retrieved S and the number of retrieved images N. Recall is calculated as the ratio between the number of relevant images retrieved and the total number of relevant images T in the database.

$$P = \frac{S}{N} \tag{22}$$

$$R = \frac{S}{T} \tag{23}$$

5.3 Retrieval Performance

In experiments, all images in the database are selected as the query images. First, we demonstrate the performance of the proposed method under different quantization levels in HSV color space and confirm the final quantization levels of H and V components. Second, we demonstrate that the improved Canberra distance is more suitable for our retrieval system. Third, the performances of proposed method are compared with other image retrieval methods.

In HSV color space, different quantization levels of H, S and V components are used to evaluate the retrieval performance of proposed method. Table 2 displays the precisions and recalls of proposed method under different quantization levels of H and V components on Corel databases.

In the experiments, the H component is set to 18, 36 and 72 bins and the V component is set to 10 and 20 bins in HSV color space. According to the retrieval results, the proposed method has best values under H 72 and S 20 on Corel databases. However, when the quantization level of color is too high, the complexity of proposed method is increased and the retrieval precision of proposed method may be decreased. Thus, we choose the vector dimension of H component as 72 and S component as 20 in HSV color space to characterize color feature.

Table 2. Precision (the number of retrieved image is 10) and recall (the number of retrieved image is 50) of the proposed method with different quantization schemes for different databases based on HSV color space. The bold values indicate the best results

Quantization level	Corel-1000		Corel-5000		Corel-10000	
	Precision (%)	Recall (%)	Precision (%)	Recall (%)	Precision (%)	Recall (%)
HSV(18_10_1416)	75.95	29.43	34.39	8.67	54.86	16.12
HSV(18_20_1416)	76.54	29.88	34.95	8.97	55.21	16.33
HSV(36_10_1416)	76.91	30.06	35.76	9.14	55.59	16.49
HSV(36_20_1416)	77.54	30.45	36.45	9.40	55.99	16.71
HSV(72_10_1416)	78.01	30.67	36.88	9.58	56.10	16.84
HSV(72_20_1416)	**78.43**	**31.05**	**37.54**	**9.83**	**56.49**	**17.04**

Four different measures (L_1 distance, L_2 distance, weighted L_1 distance and improved Canberra distance) have been used for measuring the similarity between query image and images in the database. Precision and recall of proposed method with four similarity measures have been shown in Table 3. The number of retrieved image is set from 10 to 30. Experimental results show that the improved Canberra distance is giving better results than other similarity measures. L_2 distance is not always the best metric, because it puts more emphasis on features that are greatly dissimilar. L_1 distance and weighted L_1 distance are also two common similarity measures. However, they are not suitable for proposed retrieval system although they are good similarity measures. As shown in Eq. (21), when the weight parameter is taken into account and u_x , u_y are used as smoothing factors [37, 42], the performance of proposed method is increased. So we adopt improved Canberra distance as similarity measure between images for proposed retrieval system.

Table 3. The retrieval precision and recall of the proposed method with different distance measures for Corel-1000 database

Distance measure	Precision (%)					Recall (%)				
	10	15	20	25	30	10	15	20	25	30
L_1 distance	77.73	74.39	71.94	69.64	67.64	7.77	11.16	14.39	17.41	20.29
L_2 distance	74.24	70.79	68.28	66.39	64.54	7.42	10.62	13.66	16.60	19.36
weighted L_1 distance	78.24	74.78	72.51	70.35	68.47	7.82	11.22	14.50	17.59	20.54
improved Canberra distance	**78.43**	**75.33**	**72.75**	**70.52**	**68.56**	**7.84**	**11.30**	**14.55**	**17.63**	**20.57**

Fig. 7 plots the precision-recall curves of different methods on Corel-1K database. It can be seen that the precision of the proposed method is 78.43% on Corel-1000 image database which is much better than other methods. The precisions of HSV (72-20-708) GLBP, HSV (72-20-972) GLCP, HSV (72-20-192)GCSLBP, HSV (72-20-1416) GCLBP, HSV (72-20-1416) GLTP and HSV (72-20-2124) GLMP are only 72.97%, 70.03%, 71.37%, 74.39%, 75.14% and 71.19%. We compare proposed method with other methods for each category on Corel-1000 image database to evaluate the robust performance of proposed method for image category, the number of retrieved images is set to 20. Table 4 shows the precision and recall of the proposed method for individual category on Corel-1000 database. According to Table 4 (HSV (72-20-708) GLBP, HSV(72-20-972)GLCP, HSV (72-20-192) GCSLBP, HSV (72-20-1416)GCLBP, HSV (72-20-1416) GLTP and HSV (72-20-2124) GLMP are abbreviated to GLBP, GLCP, GCSLBP, GCLBP, GLTP and GLMP), we can see that the precision and recall of the proposed method are significantly higher than other descriptors in most categories. The precision and recall of the proposed method are lower than other methods on African, dinosaur and food categories. The precision and recall of GLTP are higher than the proposed method in flower category. And the precision and recall of the proposed method are higher than GLTP, but the performance of the proposed method is lower than other methods in horse categories. Comparing with other methods, the proposed method is more robust in most categories.

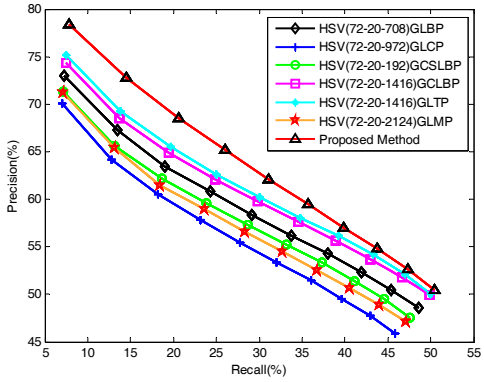

Fig. 7. The performance comparison of proposed method with other methods in terms of precision and recall on Corel-1000 database

Table 4. The individual category retrieval results of proposed method and other methods on Corel-1000 database

Category	Performance (%)	GLBP	GLCP	GCSLBP	GCLBP	GLTP	GLMP	PM
African	Precision	**72.90**	69.50	70.35	72.05	68.55	70.50	68.15
	Recall	**14.58**	13.90	14.07	14.41	13.71	14.10	13.63
Beach	Precision	37.50	32.85	33.35	38.15	42.15	34.75	**54.15**
	Recall	7.50	6.57	6.67	7.63	8.43	6.95	**10.83**
Building	Precision	56.75	54.75	55.55	55.85	53.25	55.45	**60.95**
	Recall	11.35	10.95	11.11	11.17	10.65	11.09	**12.19**
Bus	Precision	82.35	74.10	76.05	85.65	90.80	79.60	**94.35**
	Recall	16.47	14.82	15.21	17.13	18.16	15.92	**18.87**
Dinosaur	Precision	98.75	98.35	98.65	98.75	**98.80**	98.10	97.55
	Recall	19.75	19.67	19.73	19.75	**19.76**	19.62	19.51
Elephant	Precision	46.55	44.10	44.75	48.95	49.85	45.60	**64.50**
	Recall	9.31	8.82	8.95	9.79	9.97	9.12	**12.90**
Flower	Precision	72.85	68.95	78.35	78.70	**92.25**	68.55	89.25
	Recall	14.57	13.79	15.67	15.74	**18.45**	13.71	17.85
Horse	Precision	**91.65**	91.50	90.90	90.65	83.70	91.10	85.70
	Recall	**18.33**	18.30	18.18	18.13	16.74	18.22	17.14
Mountain	Precision	46.10	40.80	41.00	48.05	42.45	44.95	**48.50**
	Recall	9.22	8.16	8.20	9.61	8.49	8.99	**9.70**
Food	Precision	67.80	66.30	67.70	68.95	**70.35**	65.40	64.35
	Recall	13.56	13.26	13.54	13.79	**14.07**	13.08	12.87

On Corel-5000 image database, the precision-recall curves are illustrated in Fig. 8(a). It can be seen that the precision of the proposed method can reach 37.54%, and the precision of the proposed method is higher than other methods. Fig. 8(b) and Fig. 8(c) illustrate the individual category precision and recall of proposed method and other methods on Corel-5000 image database. We set the number of retrieved image to 10 when computing the precision and set the number of retrieved image to 50 when computing the recall. From Fig. 8(b) and Fig. 8(c), it is clear that the precision and recall of the proposed method outperform other methods in most categories on Corel-5000 image database.

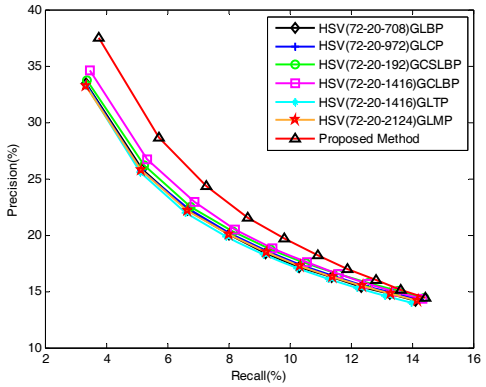

(a) Precision and recall of proposed method on Corel-5000 image database

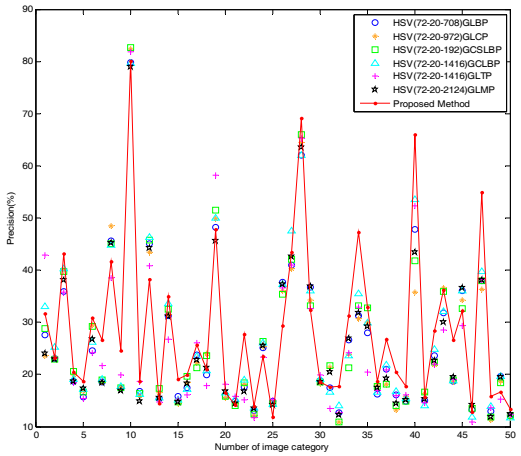

(b) Precision and image category number for each category images

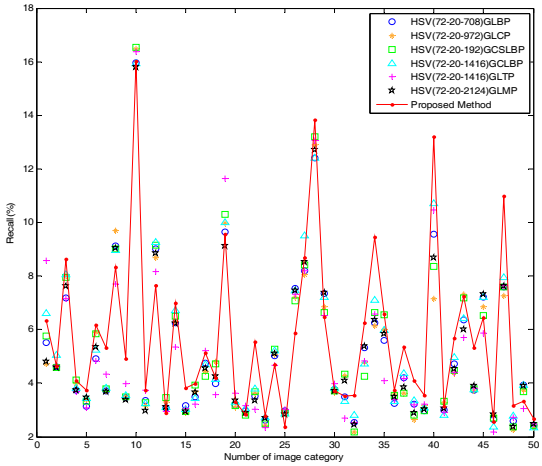

(c) Recall and image category number for each category images

Fig. 8. The retrieval performance comparison in Corel-5000 image database

On Corel-10000 image database, Fig. 9(a) plots the precision and recall curves. Fig. 9(a) shows that proposed method outperforms other methods. The precision of the proposed method is 56.50%, and precisions of other methods is less than 50%. Fig. 9(b) and Fig. 9(c) illustrate the individual category precision and recall of different methods on Corel-10000 image database. We set the number of retrieved image to 10 when computing the precision and set the number of retrieved image to 50 when computing the recall. From Fig. 9(b) and Fig. 9(c), it is clear that the precision and recall of the proposed method outperforms other methods in most categories on Corel-10000 image database.

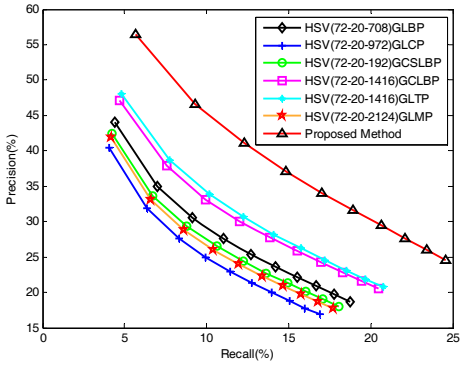

(a) Precision and recall of proposed method on Corel-10000 image database

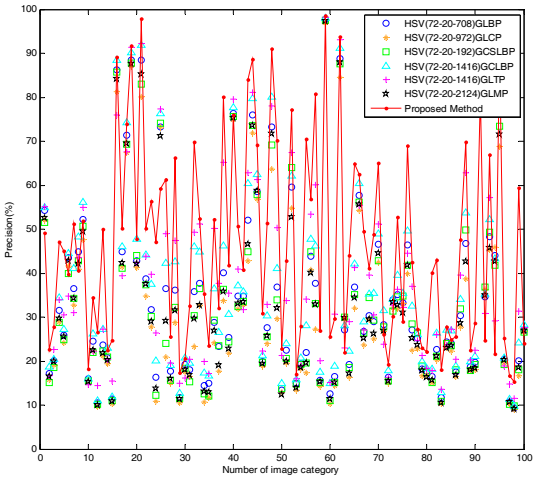

(b) Precision and image category number for each category images

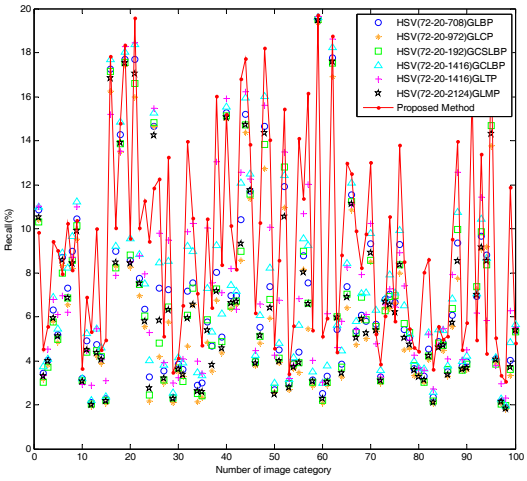

(c) Recall and image category number for each category images

Fig. 9. The retrieval performance comparison in Corel-10000 image database

Fig. 10 shows two examples of the image retrieval on Corel-10000 database by using the proposed method. In Fig. 10(a), the query image (No. 5178) is a stamp and the top 20 retrieved images using proposed method have very similar texture and color features to the query image. In Fig. 10(b), the query image (No. 3768) is a car, all the top 20 retrieved images are correct. These examples validate that the proposed method shows good discrimination power.

(a) (b)

Fig. 10. The image retrieval results (stamps and cars) of proposed method on Corel-10000 database (The top-left image is the query image)

5.4 Comparison with Other Existing Methods

We compare our method with other existing methods in terms of precision and recall on Corel-1000 database. In this experiment, we set the number of retrieved images to 20. As shown in Table 5, we can see that the proposed method is better than other methods.

Table 5. Comparison of different image retrieval methods with 20 returns on Corel-1000 database

Database	Performance (%)	Methods				
		LBP [19]	Method [43]	Method [44]	Method [45]	Proposed method
Corel-1000	Precision	61.80	58.20	72.51	57.85	**72.75**
	Recall	12.36	11.64	14.50	11.57	**14.55**

For testing of the proposed method, we compare our method with LBP and CNN. Table 6 lists the precision and recall of different methods on Corel-5000 database. The number of the retrieved images are set from 10 to 50 in this experiment. It can be seen that the proposed method is better than LBP and CNN.

Table 6. The performance comparison of different methods on Corel-5000 database

Method	Precision (%)					Recall (%)				
	10	20	30	40	50	10	20	30	40	50
LBP [19]	23.70	16.91	14.07	12.37	11.28	2.37	3.38	4.22	4.95	5.64
CNN [45]	33.18	26.34	23.11	21.00	19.50	3.32	5.27	6.93	8.40	9.75
Proposed method	**37.54**	**28.60**	**24.30**	**21.57**	**19.65**	**3.75**	**5.72**	**7.29**	**8.63**	**9.83**

We also compare our method with other existing methods in terms of precision and recall on Corel-10000 database. The number of the retrieved images is 12. According to Table 7, the precision and recall of proposed method outperform other methods.

Table 7. Comparison of different image retrieval methods with 12 returns on Corel-10000 database

Database	Performance (%)	Methods				
		LBP [19]	Method [46]	Method [47]	Method [45]	Proposed method
Corel-10000	Precision	35.84	45.24	47.25	46.67	**53.81**
	Recall	4.30	5.43	5.67	5.60	**6.46**

5.5 Discussion

LBP is invariant to monotonic intensity changes. Hence, it is robust to illumination and contrast variations. However, it is sensitive to noise and small pixel value fluctuations. LTP is more resistant to noise than LBP, but the selection of additional threshold values is not so simple. CLBP aims to preserve additional distinguishing information by using the sign descriptor, the central pixel descriptor and magnitude descriptor. However, the quantization of neighbor pixels into binary format is coarse via global threshold. CS-LBP is a modified version of the LBP feature which compared center-symmetric pairs of pixels, but it only performs well in interest region description. LCP considers the microscopic configuration and local structure information which consist of microscopic configuration modeling and LBP. Although LCP is invariant to illumination and image rotation, it is not appropriate for texture image retrieval. LMP encodes the relationship among the surrounding neighbors. Although it has good performance in biomedical image retrieval application, it has certain limitation in natural image retrieval.

LBP and LBP-like methods show impressive performance on texture analysis. However, they still have limitations. These methods disregard the co-occurrences between patterns in images. NI-CLTP is proposed to solve this problem and it considers the co-occurrence of similar ternary edges among the surrounding neighbors for a given center pixel in an image. With this method, the selection of threshold is more robust than the central pixel and the advantages of ternary pattern (the coding pattern of ternary pattern is used) and co-occurrence can be integrated. Experimental results demonstrate that the proposed method has better performance than LBP-like methods in CBIR.

5.6 Feature Vector Length

Table 8 shows the feature vector dimension of various methods. As demonstrated in Table 8, the feature vector length of proposed method is greater than $HSV(72-20-708)GLBPu2\_8\_1$, $HSV(72-20-972)$ $GLCPu2\_8\_1$ and $HSV(72-20-192)GCSLBPu2\_8\_1$, but its performance is far better than other existing methods on different databases. Fortunately, a feature size of 1508 is not a big problem for implementation. In the future work, we will reduce the feature vector dimension of proposed method and keep good retrieval precision.

Table 8. Feature vector length of various methods

Method	Feature vector length
$HSV(72-20-708)GLBPu2\_8\_1$	$72+20+12\times59=800$
$HSV(72-20-972)GLCPu2\_8\_1$	$72+20+12\times81=1064$
$HSV(72-20-192)GCSLBPu2\_8\_1$	$72+20+12\times16=284$
$HSV(72-20-1416)GCLBPu2\_8\_1$	$72+20+12\times2\times59=1508$
$HSV(72-20-1416)GLTPu2\_8\_1$	$72+20+12\times2\times59=1508$
$HSV(72-20-2124)GLMPu2\_8\_1$	$72+20+12\times3\times59=2216$
Proposed Method	$72+20+12\times2\times59=1508$

6 Conclusion

This paper proposes a novel image retrieval algorithm, namely co-occurrence local ternary patterns (CLTP) using the HSV color space. The CLTP considers neighbors intensity (NI) for a given center pixel and consequently a new operator, namely NI-CLTP, is defined. NI-CLTP encodes the intensity-based co-occurrence of local ternary edges among the surrounding neighbors for a given center pixel in eight

directions, which is different from the some existing LBP-like methods. Color feature is extracted using H and S component in HSV color space. V component is used to apply the combination of NI-CLTP and Gabor transform. The combined feature vector is applied to extract color and texture features. Extensive experimental results show that the performance of proposed method in terms of precision and recall outperform other methods on benchmark image databases.

In this paper, although the proposed image retrieval algorithm has superior performance by combining color and texture, the feature vector dimension of proposed method needs to be reduced. In the future, we plan to reduce the complexity of proposed method. Besides, the weights of color and texture are same in this paper, the bad features will affect the performance of image retrieval after combining bad and good features directly. Therefore, the weight distribution of multi-feature fusion also needs to be further studied.

Acknowledgements

The work was supported by National Natural Science Foundation of PR China (Grant no. 61370200, 61672130, 61602082), China Postdoctoral Science Foundation (2015M581331) and Science and Technology Research and Development Plan Project of Handan, Hebei Province (1721203049-1).

References

[1] Y. Rui, T.S. Huang, S.F. Chang, Image retrieval: current techniques, promising directions, and open issues, Journal of Visual Communication and Image Representation 10(1)(1999) 39-62.

[2] M.E. ElAlami, A new matching strategy for content based image retrieval system, Applied Soft Computing 14(2014) 407-418.

[3] O.A. Penatti, F.B. Silva, E. Valle, V. Gouet-Brunet, R.D.S. Torres, Visual word spatial arrangement for image retrieval and classification, Pattern Recognition 47(2)(2014) 705-720.

[4] R. Datta, D. Joshi, J. Li, J.Z. Wang, Image retrieval: ideas, influences, and trends of the new age, ACM Computing Surveys (CSUR) 40(2)(2008) 5.

[5] M.J. Swain, D.H. Ballard, Color indexing, International Journal of Computer Vision 7(1)(1991) 11-32.

[6] M.A. Stricker, M. Orengo, Similarity of color images, in: Proc. International Society for Optics and Photonics IS&T/SPIE's Symposium on Electronic Imaging: Science & Technology, 1995.

[7] J. Huang, S.R. Kumar, M. Mitra, W.J. Zhu, R. Zabih, Image indexing using color correlograms, in: Proc. IEEE Computer Society Conference on Computer Vision and Pattern Recognition, 1997.

[8] G. Pass, R. Zabih, J. Miller, Comparing images using color coherence vectors, in: Proc. of the fourth ACM International Conference on Multimedia, 1997.

[9] J.P. Jones, L.A. Palmer, An evaluation of the two-dimensional Gabor filter model of simple receptive fields in cat striate cortex, Journal of Neurophysiology 58(6)(1987) 1233-1258.

[10] C. Liu, H. Wechsler, A Gabor feature classifier for face recognition, in: Proc. the Eighth IEEE International Conference on Computer Vision, 2001.

[11] J. Han, K.K. Ma, Rotation-invariant and scale-invariant Gabor features for texture image retrieval, Image and Vision Computing 25(9)(2007) 1474-1481.

[12] R.M. Haralick, K. Shanmugam, Textural features for image classification, IEEE Transactions on Systems, Man, and Cybernetics 3(6)(1973) 610-621.

[13] C. Palm, Color texture classification by integrative co-occurrence matrices, Pattern Recognition 37(5)(2004) 965-976.

[14] A. Baraldi, F. Parmiggiani, An investigation of the textural characteristics associated with gray level cooccurrence matrix statistical parameters, IEEE Transactions on Geoscience and Remote Sensing 33(2)(1995) 293-304.

[15] L.S. Davis, S.A. Johns, J.K. Aggarwal, Texture analysis using generalized co-occurrence matrices, IEEE Transactions on Pattern Analysis and Machine Intelligence (3)(1979) 251-259.

[16] G.H. Liu, J.Y. Yang, Z. Li, Content-based image retrieval using computational visual attention model, Pattern Recognition 48(8)(2015) 2554-2566.

[17] F.R. de Siqueira, W.R. Schwartz, H. Pedrini, Multi-scale gray level co-occurrence matrices for texture description, Neurocomputing 120(2013) 336-345.

[18] P. Viola, M. Jones, Rapid object detection using a boosted cascade of simple features, in: Proc. IEEE Computer Society Conference on Computer Vision and Pattern Recognition, 2001.

[19] T. Ojala, M. Pietikainen, T. Maenpaa, Multiresolution gray-scale and rotation invariant texture classification with local binary patterns, IEEE Transactions on Pattern Analysis and Machine Intelligence 24(7)(2002) 971-987.

[20] D. Huang, C. Shan, M. Ardabilian, Y. Wang, L. Chen, Local binary patterns and its application to facial image analysis: a survey, IEEE Transactions on Systems, Man, and Cybernetics, Part C (Applications and Reviews) 41(6)(2011) 765-781.

[21] M. Heikkilä, M. Pietikäinen, C. Schmid, Description of interest regions with local binary patterns, Pattern Recognition 42(3)(2009) 425-436.

[22] X. Tan, B. Triggs, Enhanced local texture feature sets for face recognition under difficult lighting conditions, IEEE Transactions on Image Processing 19(6)(2010) 1635-1650.

[23] Y. Guo, G. Zhao, M. Pietikäinen, Texture classification using a linear configuration model based descriptor, in: Proc. British Machine Vision Conference, 2011.

[24] Z. Guo, L. Zhang, D. Zhang, A completed modeling of local binary pattern operator for texture classification, IEEE Transactions on Image Processing 19(6)(2010) 1657-1663.

[25] S. Murala, Q.J. Wu, Local mesh patterns versus local binary patterns: biomedical image indexing and retrieval, IEEE Journal of Biomedical and Health Informatics 18(3)(2014) 929-938.

[26] G.L. Shen, X.J. Wu, Content based image retrieval by combining color, texture and CENTRIST, in: Proc. 2013 Constantinides International Workshop on Signal Processing, 2013.

[27] G.H. Liu, L. Zhang, Y.K. Hou, Z.Y. Li, J.Y. Yang, Image retrieval based on multi-texton histogram, Pattern Recognition 43(7)(2010) 2380-2389.

[28] M.E. ElAlami, A novel image retrieval model based on the most relevant features, Knowledge-Based Systems 24(1)(2011) 23-32.

[29] M. Singha, K. Hemachandran, Performance analysis of color spaces in image retrieval, Assam University Journal of Science and Technology 7(2)(2011) 94-104.

[30] A. Vadivel, S. Sural, A.K. Majumdar, An integrated color and intensity co-occurrence matrix, Pattern Recognition Letters 28(8)(2007) 974-983.

[31] G.R. Cross, A.K. Jain, Markov random field texture models, IEEE Transactions on Pattern Analysis and Machine Intelligence 1(1983) 25-39.

[32] L. Liu, L. Zhao, Y. Long, G. Kuang, P. Fieguth, Extended local binary patterns for texture classification, Image and Vision Computing 30(2)(2012) 86-99.

[33] Z. Guo, L. Zhang, D. Zhang, Rotation invariant texture classification using LBP variance (LBPV) with global matching,

Pattern Recognition 43(3)(2010) 706-719.

[34] W. Zhang, S. Shan, W. Gao, X. Chen, H. Zhang, Local Gabor binary pattern histogram sequence (LGBPHS): a novel non-statistical model for face representation and recognition, in: Proc. the Tenth IEEE International Conference on Computer Vision, 2005.

[35] S. Murala, R.P. Maheshwari, R. Balasubramanian, Local tetra patterns: a new feature descriptor for content-based image retrieval, IEEE Transactions on Image Processing 21(5)(2012) 2874-2886.

[36] S. Antani, R. Kasturi, R. Jain, A survey on the use of pattern recognition methods for abstraction, indexing and retrieval of images and video, Pattern Recognition 35(4)(2002) 945-965.

[37] G.H. Liu, J.Y. Yang, Content-based image retrieval using color difference histogram, Pattern Recognition 46(1)(2013) 188-198.

[38] G.H. Liu, Z.Y. Li, L. Zhang, Y. Xu, Image retrieval based on micro-structure descriptor, Pattern Recognition 44(9)(2011) 2123-2133.

[39] J.Z. Wang, J. Li, G. Wiederhold, SIMPLIcity: Semantics-sensitive integrated matching for picture libraries, IEEE Transactions on Pattern Analysis and Machine Intelligence 23(9)(2001) 947-963.

[40] J. Li, J.Z. Wang, Automatic linguistic indexing of pictures by a statistical modeling approach, IEEE Transactions on Pattern Analysis and Machine Intelligence 25(9)(2003) 1075-1088.

[41] D. Besiris, E. Zigouris, Dictionary-based color image retrieval using multiset theory, Journal of Visual Communication and Image Representation 24(7)(2013) 1155-1167.

[42] G.N. Lance, W.T. Williams, Mixed-data classificatory programs I - agglomerative systems, Australian Computer Journal 1(1)(1967) 15-20.

[43] H.A. Jalab, Image retrieval system based on color layout descriptor and Gabor filters, in: Proc. 2011 IEEE Conference on Open Systems (ICOS), 2011.

[44] M. Subrahmanyam, Q.J. Wu, R.P. Maheshwari, R. Balasubramanian, Modified color motif co-occurrence matrix for image indexing and retrieval, Computers & Electrical Engineering 39(3)(2013) 762-774.

[45] A. Babenko, A. Slesarev, A. Chigorin, V. Lempitsky, Neural codes for image retrieval, in: Proc. European Conference on Computer Vision, 2014.

[46] G.H. Liu, J.Y. Yang, Content-based image retrieval using color difference histogram, Pattern Recognition 46(1)(2013) 188-198.

[47] S. Zeng, R. Huang, H. Wang, Z. Kang, Image retrieval using spatiograms of colors quantized by Gaussian mixture models, Neurocomputing 171(2016) 673-684.